

Strength functions, entropies and duality in weakly to strongly interacting fermionic systems

D. Angom, S. Ghosh, and V.K.B. Kota *
Physical Research Laboratory, Ahmedabad 380 009, India

We revisit statistical wavefunction properties of finite systems of interacting fermions in the light of strength functions and their participation ratio and information entropy. For weakly interacting fermions in a mean-field with random two-body interactions of increasing strength λ , the strength functions $F_k(E)$ are well known to change, in the regime where level fluctuations follow Wigner's surmise, from Breit-Wigner to Gaussian form. We propose an ansatz for the function describing this transition which we use to investigate the participation ratio ξ_2 and the information entropy S^{info} during this crossover, thereby extending the known behavior valid in the Gaussian domain into much of the Breit-Wigner domain. Our method also allows us to derive the scaling law for the duality point $\lambda = \lambda_d$, where $F_k(E)$, ξ_2 and S^{info} in both the weak ($\lambda = 0$) and strong mixing ($\lambda = \infty$) basis coincide as $\lambda_d \sim 1/\sqrt{m}$, where m is the number of fermions. As an application, the ansatz function for strength functions is used in describing the Breit-Wigner to Gaussian transition seen in neutral atoms CeI to SmI with valence electrons changing from 4 to 8.

Keywords: two-body random matrix ensemble, strongly interacting fermions, strength function, Breit-Wigner to Gaussian transition, participation ratio, information entropy, duality, CeI, SmI.

PACS numbers: 05.45.Mt, 05.30.-d, 32.30.-r, 71.23.An, 73.63.kv

I. INTRODUCTION

There are many physical systems which are statistically well described by so-called embedded ensembles of fermions, representing particles subjected to a one-body mean-field potential (defining a set of single-particle levels), and interacting with a random, two-body potential. Examples include heavy nuclei [1, 2, 3, 4], natural [5, 6], or artificial atoms (quantum dots) [7, 8], and nanometer-scale metallic grains [9]. Similar situations of randomly interacting spin systems occur in the study of spin-glass systems [10], and in the context of quantum information and quantum computation [11]. These embedded ensemble are defined as ensembles of Hamiltonians $\{H\} = h(1) + \lambda\{V(2)\}$, where $\{..\}$ denotes an ensemble distribution, $h(1) = \sum_i \epsilon_i n_i$ is a fixed one-body operator (one can also consider an ensemble $\{h(1)\}$ defined by a probability distribution $P(\epsilon_i)$ defined by the single-particle energies ϵ_i with average spacing Δ which sets the energy scale (one can thus set $\Delta = 1$ without loss of generality), and n_i is the number operator for the single-particle state $|i\rangle$. Similarly $V(2)$ is the random two-body interaction with its two-particle matrix elements chosen as independent Gaussian variables with zero center and unit variance. Thus, for m fermions in N single-particle states, $\{H\}$ is a one plus two-body random matrix ensemble (called embedded ensemble of (1+2)-body interactions[EGOE(1+2)]) [1, 2] defined by the parameters (m, N, λ) , where λ is the interaction strength. For convenience, we only consider here EGOE(1+2) for spinless fermions, but extensions to particles with intrinsic angular momentum have also been considered [7, 9, 12]. In such a case, the size of Hilbert space is given by $d = \binom{N}{m}$ and another important parameter is the connectivity K giving the number of directly coupled states as $K = 1 + m(N - m) + m(m - 1)(N - m)(N - m - 1)/4$.

Because of its broad relevance to many, a priori different, finite quantum systems, EGOE(1+2)'s have been investigated in detail by many research groups in the recent past [1, 2, 3, 7, 8, 9, 11, 12, 13, 14, 15, 16, 17, 18, 19, 20]. Most investigations used analytical methods extrapolating from the weak and the strong coupling limit, and relied on numerical calculations in the regime of intermediate values of λ . Focusing on the statistical spectral and wavefunction properties, the dominant features of EGOE(1+2) that emerged from those investigations can be summarized as:

1. There is a marker λ_c , such that for $\lambda > \lambda_c$ the many-body level spacing distribution becomes close to that of the Gaussian Orthogonal Ensemble (GOE) of random matrices [21], while for $\lambda < \lambda_c$ the level fluctuations are close to Poisson. It was further established that $\lambda_c \propto 1/m^2 N$ [15, 16]; specifically for $m = 6$ and $N = 12$, $\lambda_c \simeq 0.06$ [1].
2. As λ increases from $\lambda = 0$, the strength function (to be defined below in Section 2) undergoes a crossover from a delta-peak, first to a Breit-Wigner (BW), then to a Gaussian form. Related to that crossover, there are

two markers $\lambda_F^{(1,2)}$ such that, for $\lambda_F^{(1)} \leq \lambda \leq \lambda_F^{(2)}$, the strength function is well approximated by a BW form [1, 3, 13, 14, 17, 18, 19]; the BW form emerges above $\lambda_F^{(1)}$, which is exponentially smaller in m and N than λ_c . In particular, the BW form occurs while the spectral fluctuations are still Poissonian. The $\lambda > \lambda_F^{(2)}$ region (with full GOE spectral and wavefunction properties) is called the Gaussian domain [3]. From now on we put $\lambda_F = \lambda_F^{(2)}$; note that $\lambda_F \gg \lambda_c$. Arguments based on BW spreading widths give $\lambda_F \propto 1/\sqrt{m}$ [14, 19]; for the specific case $m = 6$ and $N = 12$, $\lambda_F \simeq 0.2$ [3].

3. In the Gaussian domain, the participation ratio (PR) ξ_2 and the exponential of the information entropy ($\exp[S^{\text{info}}(E)]$) (both quantities will be defined in Section 3 below) take Gaussian forms when plotted as a function of the energy [3]. The variances of these Gaussian are $(1 + \zeta^2)/(2\zeta^2)$ and $1/\zeta^2$ respectively, where $\zeta^2 = \sigma_h^2(m)/[\sigma_h^2(m) + \lambda^2\sigma_V^2(m)]$; $\sigma_h(m)$ is the spectrum width produced by $h(1)$ in the total m -particle space and similarly $\sigma_V(m)$ is the width produced by $V(2)$. Also, in the BW region, the PR is given by the ratio of the spreading width and the spacing between directly (by $V(2)$) connected states and $S^{\text{info}} \sim \ln(\text{PR})$ [17] (see also [22]).
4. There is a fourth marker λ_d such that at $\lambda = \lambda_d$ the strength functions, PR and S^{info} expressed in either the $h(1)$ (i.e. $\lambda = 0$) and $V(2)$ (i.e. $\lambda = \infty$) basis will coincide. This is accompanied by a duality transformation relating the values of those quantities in the $h(1)$ basis to those in the $V(2)$ basis by $\lambda \rightarrow \lambda_d^2/\lambda$ [19]. In Section 5 the (m, N) dependence of λ_d will be shown to be $\lambda_d \sim 1/\sqrt{m}$ (correcting the previously postulated result $\lambda_d \sim 1/m^{1/4}$ [19]); for $m = 6$ and $N = 12$, as we see ahead, $\lambda_d \simeq 0.3$.

In addition, another important result for EGOE(1+2) is that the smoothed (ensemble averaged) density of states takes on a Gaussian form independently of λ [1, 2, 23]. Our purpose in this paper is to bring completion to the investigations related to the points (1)-(4) above. In particular, we will introduce an interpolating function for strength functions for the BW to Gaussian transition and apply it to neutral CeI to SmI atoms. Now we will give a preview.

In Section 2 we discuss a variant of the well known Student's t-distribution [24] (hereafter called $F_{k:BW-G}(E)$) and show that it is well suited for describing the BW to Gaussian transition, as a function of one parameter α . Numerical calculations allow to establish a one-to-one correspondence between α and the interaction strength λ . In Section 3, the resulting $F_{k:BW-G}(E)$ is used to calculate both PR and S^{info} , and comparison is made with direct numerical calculations of these quantities as a function of λ , over the full range of variation of λ , thereby extending previous similar investigations which were restricted to either the Gaussian [3] or BW [17, 19] domains. Additional structures in the wave functions can be captured by the structural entropy $S_{\text{str}} \equiv S^{\text{info}} - \ln \xi_2$, which measures the amount of information contained in the tails of the strength functions. Results of an analysis of S_{str} is also given in Section 3. In Section 4, the $F_{k:BW-G}(E)$ is applied in the analysis of the BW to Gaussian transition one observes as we go from neutral CeI atom to SmI atom. In Section 5, the existence of a duality transformation in EGOE(1+2) (which was established in Ref. [19]) is discussed and it is shown that, using the results for PR and S^{info} in the Gaussian domain, the duality point $\lambda_d \sim 1/\sqrt{m}$. Conclusions and final comments are given in Section 6.

II. INTERPOLATING FUNCTION FOR BW TO GAUSSIAN TRANSITION IN STRENGTH FUNCTIONS

Given the mean-field $h(1)$ basis states $|k\rangle$ and the expansion of the eigenstates $|E\rangle$ as $|E\rangle = \sum_k C_k^E |k\rangle$, the strength function $F_k(E)$ is defined by

$$F_k(E) = \sum_{E'} \left| C_k^{E'} \right|^2 \delta(E - E') = \langle |C_k^E|^2 \rangle (d \rho^H(E)) \quad (1)$$

In Eq. (1), $\langle \dots \rangle$ indicates an ensemble average, $d = \binom{N}{m}$ is the m -particle space dimension and $\rho^H(E)$ is the normalized (and ensemble averaged) density of states. As mentioned in Section 1, $\rho^H(E)$ is in general a Gaussian (often the superscript H is dropped),

$$\rho^H(E) = \frac{1}{\sqrt{2\pi} \sigma_H(m)} \exp -\frac{\hat{E}^2}{2}; \quad \hat{E} = (E - \epsilon_H(m))/\sigma_H(m) \quad (2)$$

where $\epsilon_H(m) = \langle H \rangle^m$ is the spectrum centroid and similarly $\sigma_H(m)$ is the spectral width. The BW and Gaussian (denoted by \mathcal{G}) forms of $F_k(E)$ are,

$$F_{k:BW}(E) = \frac{1}{2\pi} \frac{\Gamma_k}{(E - E_k)^2 + \Gamma_k^2/4}, \quad F_{k:\mathcal{G}}(E) = \frac{1}{\sqrt{2\pi} \sigma_k} \exp - \frac{(E - E_k)^2}{2\sigma_k^2} \quad (3)$$

where $E_k = \langle k|H|k \rangle$. With $p = \int_{-\infty}^{\mathcal{E}_p} F_k(E) dE$, the spreading width $\Gamma_k = \mathcal{E}_{3/4} - \mathcal{E}_{1/4}$. Similarly the variance of F_k is $\sigma_k^2 = \langle k|H^2|k \rangle - (\langle k|H|k \rangle)^2$. Expressions for Γ_k and σ_k in terms of (m, N, λ) are given in Sections 5 and 3 respectively. Both spreading width Γ_k of the BW and σ_k of the Gaussian strength functions are essentially independent of k (provided one considers energies not too far away from the center of the density of states) [1, 3, 13]. Simultaneously, the energies E 's (of H) and E_k 's will have the same centroid. Moreover, just as the state density $\rho^H(E)$, the E_k 's density (denoted by $\rho^{H_k}(E_k)$) is also a Gaussian. These results are used throughout this paper and without loss of generality the centroids of E 's and E_k 's are set equal to zero. As it is discussed in detail in [3], the width of $\rho^{H_k}(E_k)$ is essentially due to $h(1)$ (with a small correction from $V(2)$ as explained in the Appendix in [3]) and σ_k is generated by $V(2)$. Before proceeding further it should be mentioned that the strength functions are basis dependent and one can define strength functions in the $V(2)$ basis also. We will turn to this question when discussing duality transformation in Section 5.

For the BW to Gaussian transition we make the following ansatz for $F_k(E)$

$$F_{k:BW-\mathcal{G}}(E : \alpha, \beta) dE = \frac{(\alpha\beta)^{\alpha-\frac{1}{2}} \Gamma(\alpha)}{\sqrt{\pi} \Gamma(\alpha - \frac{1}{2})} \frac{dE}{((E - E_k)^2 + \alpha\beta)^\alpha}, \quad \alpha \geq 1 \quad (4)$$

The $F_{k:BW-\mathcal{G}}$ in (4) gives BW for $\alpha = 1$ and Gaussian for $\alpha \rightarrow \infty$ (this can easily be checked using Stirling's approximation). As required, it is normalized to unity for any positive value of the continuous parameter α . For $2\alpha - 1$ a integer, $F_{k:BW-\mathcal{G}}$ gives the so called *Student's t-distribution* [24], which is well known in statistics. In particular, the *Student's* distribution $f(x)$ with a parameter ν given in Table 5.7 of [24] reduces to (4) with the change $\alpha = (\nu + 1)/2$, ν a positive integer, and $x \rightarrow \sqrt{\frac{2\nu}{\nu+1}} (E - E_k)/\sqrt{\beta}$. Note that the construction of $F_{k:BW-\mathcal{G}}$ in Eq. (4) is similar in spirit to the Brody distribution, interpolating between the Poisson and Wigner-Dyson distributions for nearest neighbor spacing distribution (NNSD) [2]. Also, just as some groups use for the NNSD a linear combination of Poisson and Wigner forms multiplied by x and $(1 - x)$ respectively with x being the mixing parameter, it is possible to use $\mu F_{k:BW}(E) + (1 - \mu) F_{k:\mathcal{G}}(E)$ for the BW to Gaussian transition with μ ($0 \leq \mu \leq 1$) being the mixing parameter. This simple form is not explored in this paper as it is unlikely that a theory for strength functions for EGOE(1+2) will give this form.

In $F_{k:BW-\mathcal{G}}(E : \alpha, \beta)$, the parameter α is sensitive to shape changes, while the parameter β supplies the energy scale over which $F_{k:BW-\mathcal{G}}(E : \alpha, \beta)$ extends. Since we focus on the shape transformation, α is the significant parameter. First, it is easy to see that $F_{k:BW-\mathcal{G}}(E : \alpha, \beta)$ is an even function of $E - E_k$, so that all of its finite odd cumulants vanish (strictly speaking, the centroid is E_k only for $\alpha > 1$; see [24]). The variance of $F_{k:BW-\mathcal{G}}$, defined only for $\alpha > 3/2$, is

$$\sigma^2(F_{k:BW-\mathcal{G}}) = \left(\frac{\alpha}{2\alpha - 3} \right) \beta, \quad \alpha > 3/2. \quad (5)$$

and it is useful to recall that $\sigma^2(F_k) = \lambda^2 \sigma_V^2$ [3]. For $\alpha > 3/2$ one can use (5) to fix β while for $\alpha \leq 3/2$, it is the spreading width Γ (this is well defined for all α values) that is useful for fixing the β value. There is no simple expression for Γ as a function of α and β but using (4) this can be calculated numerically. Just as Eq. (5), the excess parameter (also known as Kurtosis) of $F_{k:BW-\mathcal{G}}$ is $\gamma_2 = 6/(2\alpha - 5)$ for $\alpha > 5/2$. However this expression is not useful in practice as the spectrum is always of finite range and this causes large deviations for $\alpha \approx 2 - 8$. Therefore it is more useful to consider γ_2 with the spectrum ranging say from $-a$ to $+a$. Then Eq. (4), with proper normalization, gives,

$$\gamma_2(a : \alpha, \beta) = \frac{9}{5} \frac{{}_2F_1(\frac{5}{2}, \alpha; \frac{7}{2}; -\eta^2) {}_2F_1(\frac{1}{2}, \alpha; \frac{3}{2}; -\eta^2)}{[{}_2F_1(\frac{3}{2}, \alpha; \frac{5}{2}; -\eta^2)]^2} - 3 \quad (6)$$

where $\eta^2 = (a^2/\alpha\beta)$, and ${}_2F_1$ a hypergeometric function.

In Fig. 1 the results of EGOE(1+2) for $F_k(E)$ are compared, for the $m = 6$, $N = 12$ system at $E_k = 0$ (i.e. in the middle of the band), with the best fit $F_{k:BW-G}$ for various values of λ . In the fits, the β values are fixed using Eq.(5) for $\lambda \geq 0.1$ (for these, $\alpha > 1.6$) and the spreading width Γ is used ($\beta \sim \Gamma^2/4$) for $\lambda = 0.06$ (here $\alpha = 1.2$). In the fits, also imposed is the condition that the value of γ_2 calculated from Eq. (6) over the spectrum range should be close to the numerical EGOE(1+2) values. As it is seen from Fig. 1, the fits are excellent over a wide range of λ values; in the calculations only $\lambda \geq 0.06$ are considered (for the system considered in Fig. 1, $\lambda_c \sim 0.06$). The variation of α with λ is shown in Fig. 2. The parameter α raises slowly upto λ_F (note that $\lambda_F \sim 0.2$ for the EGOE(1+2) system used in Fig. 1 [3]) and then it starts rising sharply with λ . Finally the α values start saturating after $\lambda > \lambda_0 = 0.3$ (the saturation is artificial as determination of α for $\lambda \gg \lambda_0$ is difficult as here $F_k(E)$ will be very close to Gaussian). The criteria $\alpha \sim 4$ and $\gamma_2 \sim 1$ appear to define λ_F . Fig. 2 shows that the BW to Gaussian transition is a sharp transition and therefore studies in BW and Gaussian regimes can be carried out independently, to a good approximation, as it is done in many papers before. Now we will apply $F_{k:BW-G}$ to study PR and S^{info} in the region intermediate to BW and Gaussian forms.

III. PARTICIPATION RATIO AND INFORMATION ENTROPY IN THE BW TO GAUSSIAN TRANSITION REGION

Two important measures of the complexity of eigenstates of interacting systems are the participation ratio and information entropy. As in the previous section, we expand the Hamiltonian eigenstates in the noninteracting mean-field basis as $|E\rangle = \sum_k C_k^E |k\rangle$. Then PR and information entropy are defined as

$$\begin{aligned} \xi_2(E) &= \left\{ \sum_k |C_k^E|^4 \right\}^{-1}, \\ S^{info}(E) &= - \sum_k |C_k^E|^2 \ln |C_k^E|^2. \end{aligned} \quad (7)$$

The subscript ‘2’ denotes that ξ_2 is the second Rényi entropy [25]. Qualitatively, ξ_2 counts the number of $\{|k\rangle\}$ -basis components necessary to construct one typical $|E\rangle$ -state, and is thus often referred to as the Number of Principal Components (NPC). Obviously, both ξ_2 and S^{info} are basis dependent, and could as well be defined starting from another expansion. Eq. (7) gives their expression with respect to the $h(1)$ basis (i.e. the $|k\rangle$'s in Eq. (7), as in Section 2, are $h(1)$ basis states), consequently, ξ_2 and S^{info} give measures of the spreading of eigenstates over the noninteracting basis as the many-body interaction is made stronger and stronger. Below, in Section 5, we will deal with these measures defined with respect to the $V(2)$ basis. Following Ref. [3] one can write ξ_2 and S^{info} in terms of the strength functions,

$$\begin{aligned} \{\xi_2(E)/\xi_2^{GOE}\}^{-1} &= \frac{1}{[\rho^H(E)]^2} \int_{-\infty}^{\infty} dE_k \rho^{H_k}(E_k) [F_k(E)]^2, \\ S^{info}(E) - S_{GOE}^{info} &= - \frac{1}{\rho^H(E)} \int_{-\infty}^{\infty} dE_k \rho^{H_k}(E_k) F_k(E) \ln \frac{F_k(E)}{\rho^H(E)}. \end{aligned} \quad (8)$$

An obvious notation refers to the GOE values,

$$\begin{aligned} \xi_2^{GOE} &= d/3, \\ \exp(S_{GOE}^{info}) &= 0.48d. \end{aligned} \quad (9)$$

In the Gaussian domain, with $F_k(E)$ being a Gaussian with centroid at E_k and width $\lambda\sigma_V(m)$, the integrals in Eq. (8) are easy to evaluate (note that $\rho^H(E)$ and $\rho^{H_k}(E_k)$ are zero centered Gaussians with width $\sigma_H(m)$ and $\sigma_h(m)$ respectively) and they give [3],

$$\begin{aligned} \xi_2(E)/\xi_2^{GOE} &= \sqrt{1-\zeta^4} \exp - \frac{\zeta^2 \hat{E}^2}{1+\zeta^2}, \\ \exp(S^{info}(E) - S_{GOE}^{info}) &= \sqrt{1-\zeta^2} \exp \frac{\zeta^2}{2} \exp - \frac{\zeta^2 \hat{E}^2}{2}. \end{aligned} \quad (10)$$

The important parameter in Eq. (10) is the correlation coefficient ζ . For ξ_2 and S^{info} in $h(1)$ ($\lambda = 0$) basis $\zeta \equiv \zeta_0$ where

$$\left(\zeta_0^{(m)}\right)^2 = \frac{\sigma_h^2(m)}{\sigma_h^2(m) + \lambda^2 \sigma_V^2(m)} \quad (11)$$

Strictly speaking $\sigma_h^2(m)$ in the numerator should be replaced by the variance of E_k energies and similarly the denominator by $\sigma_H^2(m)$. Eq.(11) is obtained by recognizing that the former is very close to σ_h^2 and the later is essentially $\sigma_h^2 + \lambda^2 \sigma_V^2$. In fact these results are valid in the dilute limit ($m \rightarrow \infty$, $N \rightarrow \infty$, $m/N \rightarrow 0$) and here h and V are orthogonal. Even away from the dilute limit they remain to be good approximations (see Fig. 3 ahead for a test). Propagation formulas [1] for $\sigma_h^2(m)$ and $\sigma_V^2(m)$ are

$$\begin{aligned} \sigma_h^2(m) &= \frac{m(N-m)}{(N-1)} \sigma_h^2(1) = f^2 \Delta^2 \\ \lambda^2 \sigma_V^2(m) &= \frac{m(m-1)(N-m)(N-m-1)N(N-1)}{(N-2)(N-3)} \frac{\lambda^2}{4} = g^2 \lambda^2 \end{aligned} \quad (12)$$

It is always possible to write $\sigma_h^2(1)$ in terms of Δ^2 and for example for a uniform single particle spectrum,

$$\sigma_h^2(1) = (N+1)(N-1) \frac{\Delta^2}{12} \quad (13)$$

As shown in Fig. 3 (for the $m = 6, N = 12$ system), results of the formulas (11,12) agree very well with numerical EGOE(1+2) values for ζ_0 .

Substituting the interpolating $F_{k:BW-G}(E)$ for $F_k(E)$ in Eq. (8), one can study ξ_2 and S^{info} as a function of λ . The integral in Eq. (8) for ξ_2 can be simplified for $E = 0$ and this gives (for $\alpha > 3/2$),

$$\begin{aligned} \xi_2(E=0)/\xi_2^{GOE} &= \\ \left\{ \sqrt{\frac{2}{(2\alpha-3)}} \frac{\Gamma^2(\alpha)}{\Gamma^2(\alpha-\frac{1}{2})} \frac{1}{\sqrt{\zeta^2(1-\zeta^2)}} U\left(\frac{1}{2}, \frac{3}{2} - 2\alpha, \frac{(2\alpha-3)(1-\zeta^2)}{2\zeta^2}\right) \right\}^{-1} \end{aligned} \quad (14)$$

where $U(- - -)$ is hypergeometric-U function [26]. The corresponding result in the Gaussian domain (from Eq. (10)) is $\sqrt{1-\zeta^4}$. In deriving Eq. (14), we used Eqs. (5) and (11) for eliminating β and simplifying all the variances into ζ^2 . It is important to note that Eq. (14) is valid only for $\alpha > 3/2$ as (5) is used in deriving this formula. For $\alpha \leq 3/2$ a compact formula could not be derived but one can use (8) for numerical evaluations. Similarly, in the case of $S^{\text{info}}(E=0)$ a simple formula like Eq. (14) could not be obtained for any α and once again here one can use (8) for numerical evaluations. For $\xi_2(E=0)$ results from (14) for $\lambda \geq 0.08$ and the result from (8) for $\lambda = 0.06$ are compared with numerical EGOE(1+2) calculations for the $m = 6, N = 12$ system in Fig. 4. In these calculations the α -values are read off from Fig. 2 and ζ^2 from Fig. 3. Comparing with the Gaussian domain results given by (10), it is seen that they are good for $\lambda > \lambda_F$ as expected; these results again confirm that $\lambda_F \sim 0.2$ for the $m = 6, N = 12$ system. The agreement between (14,8) and the numerical calculations continue upto $\lambda \sim 0.06$. For $\lambda < \lambda_F$ as the BW structure is more dominant, there will be more localization and hence ξ_2 decreases fast as λ is decreasing as seen in Fig. 4; finally they will approach zero for $\lambda \rightarrow 0$. The results based on (8) will not extend to the region $\lambda \lesssim \lambda_c$ as here the GOE assumptions used in deriving these equations (see [3]) will fail. Finally, for $S^{\text{info}}(E=0)$ the results are similar to those shown in Fig. 4. This is not surprising as in many numerical calculations (including the present calculations) it is seen that $S^{\text{info}}(E) \sim \ln(\xi_2(E))$ and therefore only their difference can capture the information not contained in the bulk of S^{info} or PR. With this clue, recently it is argued [25] that the structural entropy $S_{\text{str}}(E) = S^{\text{info}}(E) - \ln(\xi_2(E))$ is an important measure of complexity (in addition to $S^{\text{info}}(E)$ or $\xi_2(E)$) in eigenfunctions. More importantly S_{str} is free of divergences associated with S^{info} and PR. Note that $\exp(S_{\text{GOE}}^{\text{info}})$ and ξ_2^{GOE} are $0.48d$ and $d/3$ respectively and therefore they diverge as the matrix dimension $d \rightarrow \infty$. For interacting particle systems it is observed that $S_{\text{str}}(E=0)$ vs λ (or the disorder in the Anderson model[25]) exhibits a peak. It is then of interest to examine S_{str} in terms of the results given Section 2. First we consider S_{str} in the BW and Gaussian domains.

For small λ , one can estimate S_{str} using the the BW approach, i.e. taking $F_{k:BW}$ from Eq.(3), and using $\langle |C_k^E|^2 \rangle = F_{k:BW}(E)\Delta_m$, where Δ_m gives the many-body level spacing. Inserting this into Eq.(7) and replacing the sums by integrals over E_k one then gets, by restricting to $E = 0$,

$$S_{\text{str}}(0) = \frac{1}{\pi} \int_{-\tan a}^{\tan a} d\epsilon \frac{\ln(1 + \epsilon^2)}{1 + \epsilon^2} + \ln \left[\frac{2a + \sin 2a}{2\pi} \right] + \ln \left[\frac{\pi\Gamma}{2\Delta_m} \right] \left(\frac{2a}{\pi} - 1 \right), \quad a = \arctan(2B/\Gamma) \quad (15)$$

where B is the many-body bandwidth and $\Gamma \propto \lambda^2$ is the BW width. The upper limit $S_{\text{str}}(0) \rightarrow \ln 2 \sim 0.7$ follows by letting $B/\Gamma \rightarrow \infty$ (then $a \rightarrow \pi/2$) in (15). With Γ increasing with increasing λ , the $S_{\text{str}}(0)$ starts decreasing from the maximum value. Similarly, in the Gaussian domain, using (10), one has

$$S_{\text{str}}(0) = \ln(1.44) + \frac{1}{2} (\zeta^2 - \ln(1 + \zeta^2)) \quad (16)$$

It should be noted that $S_{\text{str}}^{GOE} \simeq \ln(1.44)$ independent of E . An interesting observation (though its significance is not clear) is that for $\lambda = 0$ (then $\zeta = 1$) the S_{str} is sum S_{str} for GOE and a Gaussian; note that for a Gaussian distribution, as shown in [25], $S_{\text{str}} = \frac{1}{2}(1 - \ln 2)$. As $\lambda \rightarrow \infty$ gives $\zeta = 0$, S_{str} starts from GOE value (0.3689) for very large λ and then starts increasing with decreasing λ .

For the intermediate regime and for $\lambda \leq \lambda_c$ no analytical results could be derived yet but numerical calculations give some insight. Fig. 5 shows the EGOE(1+2) results for $S_{\text{str}}(E = 0)$ vs λ in the $h(1)$ basis and their comparison with the results from (8,14) where $F_{k:BW-G}$ given by (4) is used. The S_{str} is well described for $\lambda \gg \lambda_c$ and for the $m = 6, N = 12$ system considered in Fig. 5 the theory given by (8,14) is good upto $\lambda = 0.1$. Comparing with Eqs. (15,16), it is seen that the Gaussian domain result (16) describes the results for $\lambda \geq \lambda_F$ while the BW result (15) describes only the trends for λ between 0.1 and λ_F (with the maximum possible value for S_{str} being 0.7). More importantly, as seen from Fig. 5 and also from Fig. 4 of [19], S_{str} exhibits a peak around a λ value not far from λ_c marker and here the level fluctuations will have Poisson component. Thus it is plausible that the peak arises due to large spectral(and strength) fluctuations. A good theory for S_{str} generating the observed peak is at present not available.

IV. BW TO GAUSSIAN TRANSITION IN NEUTRAL ATOMS CEI TO SMI

Realistic examples for the BW to Gaussian transition in strength functions are expected to come from neutral lanthanide atoms. It is known from the analysis of CeI by Flambaum et al [5] and PrI by Cummings et al [27] that the $F_k(E)$ for these atoms with 4 and 5 valance electrons respectively are close to BW while those of SmI with 8 valance electrons, as shown in [6], are close to Gaussian. This series of atoms is completed by NdI and PmI with 6 and 7 valance electrons. We made calculations for not only NdI and PmI but also for the other three by using the same method and this is briefly discussed below before giving the results. Also let us add that as $\lambda_F \propto 1/\sqrt{m}$, it is to be expected that, with m changing from 4-8, there should be BW to Gaussian transition with H fixed. This is indeed confirmed by the results discussed ahead.

The ground state configurations of Ce, Pr, Nd, Pm and Sm are $4f^5d6s^2(^1G_4)$, $4f^36s^2(^4I_{9/2})$, $4f^46s^2(^5I_4)$, $4f^56s^2(^6H_{5/2})$ and $4f^66s^2(^7F_0)$ respectively. Coupling of the $5d$ and $4f$ valance electrons produce several configurations and indicate strong configuration mixing. Previous work on Sm I [28] and lanthanide series [29] have established that an appropriate method of calculation is the multiconfiguration Dirac-Fock (MCDF) [30], where an atomic state function (ASF) $|\bar{\Gamma}PJM\rangle$ is approximated as a linear combination of configuration state functions (CSFs) $|\gamma PJM\rangle$. That is $|\bar{\Gamma}PJM\rangle = \sum_k c_k |\gamma_r PJM\rangle$, where c_k s are the mixing coefficients, P , J and M are parity, total angular momentum and magnetic quantum numbers respectively, and $\bar{\Gamma}$ and γ_k are additional quantum numbers to define each of the ASFs and CSFs uniquely. The CSFs are linear combinations of Slater determinants and ASFs are eigenfunctions of the Dirac-Coulomb Hamiltonian H^{DC} [30]. In the present study, a series of extended optimized level(EOL)-MCDF calculations are carried out using GRASP92 [31] to generate a single electron basis set consisting of $(1-6)s_{1/2}$, $(2-6)p_{1/2}$, $(2-6)p_{3/2}$, $(3-5)d_{3/2}$, $4f_{5/2}$ and $4f_{7/2}$ orbitals. The EOL-MCDF orbitals are less state specific compared to ground state extremization and suitable for studying spectral properties and structure of ASFs. Then a CSF space of a specific J having single and double excitations from a reference configuration $4f^l 5d^m 6s^2$ to $5d$, $6p$ and $4f$ shells, where l and m are the occupancy of the shells is generated. This sequence of calculations is

TABLE I: Details of the angular momentum, the reference configuration considered and the number of CSFs generated for each of the atoms. The numbers within parenthesis are the number of CSFs chosen for the final calculations.

Element	J^P	Ref Config	Number of CSFs
Ce	4^-	$4f5d6s^2$	373 (308)
Pr	$9/2^-$	$4f^36s^2$	1378 (1278)
Nd	4^+	$4f^46s^2$	2200 (2000)
Pm	$9/2^-$	$4f^56s^2$	4378 (4178)
Sm	4^+	$4f^66s^2$	7325 (6500)

repeated for each of the atoms. Details of the J^P and the reference configuration considered and the number of CSFs generated for each of them are given in Table I. Note that the parity (P) is chosen to be same as that of the the ground state and J is 4 for even and $9/2$ for odd cases. ASFs and corresponding eigenvalues within the CSF space considered are obtained by a configuration interaction calculation. For further analysis related to the structure of the ASFs, we choose CSFs which have close to uniform separation of $H_{kk}^{\text{DC}} = \langle \gamma_k P J M | H^{\text{DC}} | \gamma_k P J M \rangle$. For example, in Sm only 6500 of the 7325 CSFs generated are considered, the first 200 and last 625 CSFs are excluded. Then, the strength function $F_k(E) = \sum_{E'} |c_k^{E'}|^2 \delta(E - E')$ of the selected CSFs are calculated, where c_k^E is the mixing coefficient of $|\gamma_k P J M\rangle$ for the ASF having eigenvalue E . To get a representative $\bar{F}_k(E)$ we calculate the average of $F_k(E)$ s around the centroid and over 3% of the range of H_{kk}^{DC} , i.e. average strength functions with $E_k = 0$.

Calculated average strength functions (with $E_k = 0$) are compared with the best fit $F_{k:BW-G}(E)$ in Fig. 6. In the fits, Eq. (5) is used to eliminate β . The α values for each atom are given in the figure. Firstly it is seen that $F_{k:BW-G}(E)$ gives excellent description of the calculated strength functions and the BW to Gaussian transition is clearly seen in Fig. 6 with α changing from 1.85 to 14 as we go from CeI to SmI. The calculated γ_2 values are also consistent with this transition as they change from 6.44 to 0.46. Comparing with Fig. 1, CeI and PrI atoms are close to $\lambda \sim 0.1 - 0.15$ cases (F_k is close to BW), NdI and PmI are close to $\lambda \sim 0.2 - 0.25$ cases (F_k is intermediate to BW and Gaussian) and SmI is close to $\lambda \sim 0.3$ case (F_k is close to Gaussian) of the $m = 6, N = 12$ EGOE example. For further confirming the BW to Gaussian transition the $\xi_2(E = 0)/\xi_2^{\text{GOE}}$ values are calculated using Eq. (14) and the deduced α values (used also are the calculated ζ values). They change from 0.21 to 0.6 for CeI to SmI. These EGOE(1+2) numbers are close to $\xi_2(E = 0)/\xi_2^{\text{GOE}}$'s generated by the calculated atomic eigenstates. However there are large fluctuations in $\xi_2(E)$, as the atomic calculations produce in general, for many states, more localization than expected from EGOE(1+2); if we average $\xi_2(E)$ in the neighborhood of $E = 0$, then the calculated values are $\sim 20 - 30\%$ smaller than the values given by Eq. (14). This is already seen in CeI and PrI in [27] and SmI in [6]. The present calculations confirm this to be a generic behavior. The source of this localization and modifications of EGOE(1+2) for incorporating this property will be discussed elsewhere. Here it suffices to conclude that, from the results in Fig. 6, CeI to SmI unmistakably exhibit BW to Gaussian transition for $E_k = 0$.

V. DUALITY BETWEEN WEAK AND STRONG MIXING LIMITS

For each realization of the Hamiltonian $H = h(1) + \lambda V(2)$, two asymptotic natural basis emerge: the noninteracting basis defined by h , and the $\lambda = \infty$ basis defined by V . The previous discussions in Sections 2 and 3 were concerned with strength functions, PR and S^{info} in the noninteracting basis only. Here we extend this discussion to the $\lambda = \infty$ basis, and will focus on the existence of a duality transformation between the two basis, following the recent work of Jacquod and Varga (JV) [19]. JV found that a *duality* point λ_d exists where all the statistical wavefunction properties in these two basis coincide, and that the wavefunction properties in the noninteracting ($\lambda = 0$) basis are related to those in the $\lambda = \infty$ (fully interacting) basis by a duality transformation $\lambda \leftrightarrow \lambda_d^2/\lambda$. An ambiguity in JV results lied with the fact that the existence and scaling of the duality point λ_d were derived within the BW approximation, while λ_d explicitly lies outside the BW regime. We therefore extend those theoretical arguments by similar ones in the Gaussian approximation, but first recall JV results.

In the noninteracting basis, and in the BW regime, the strength functions will have Lorentzian shape. To estimate its width via the golden rule, one first has to realize that there are, beside the one-body spacing Δ , two important

energy scales [15] : the mean spacing between states directly coupled by the two-body interaction $\Delta_c^{(0)} = B_2^{(0)}/K \approx 4\Delta/Nm^2$ and the m -body spacing $\Delta_m^{(0)} = B_m^{(0)}/d$, where $B_m^{(0)} \approx \sqrt{m}N\Delta$ is the m -body band (note that $B_m^{(0)} \sim \sigma_h(m)$ with $\sigma_h(m)$ given by (12,13)). Note that this estimate slightly differs from that of JV where the m -body bandwidth $B_m^{(0)}$ was approximated by the extremal possible energy values, instead of the rms of the density of states. Then, the width of the BW strength function is approximated via the golden rule as $\Gamma^{(0)} \propto \lambda^2/\Delta_c^{(0)} \sim \lambda^2Nm^2/\Delta$. Finally, in the dilute limit $m \ll N$, the PR is obtained as $\xi_2^{(0)} = \Gamma^{(0)}/\Delta_m^{(0)} \propto \lambda^2m^{3/2}d/\Delta^2$. Note that, this result differs from the JV estimate given in [19] by the factor $m^{3/2}$ instead of m . As is the case for $\Gamma^{(0)}$, the Golden rule gives a good estimate of the width $\Gamma^{(\infty)}$ of the strength functions expressed in the $\lambda = \infty$ basis, in the BW regime. Following JV, it is seen that $\Gamma^{(\infty)} \sim m(N-m)\Delta^2/\lambda$, and one gets the PR in the $\lambda = \infty$ basis as $\xi_2^{(\infty)} = \Gamma^{(\infty)}/\Delta_m^{(\infty)} \propto (\Delta/\lambda)^2d$. The duality point is then defined by $\xi_2^{(0)}(\lambda_d) = \xi_2^{(\infty)}(\lambda_d)$ which gives the parametric dependence

$$\lambda_d \propto \Delta/m^{3/8}. \quad (17)$$

This result [32] is in better agreement with the numerical data presented by JV, where it was found that $\lambda_d \sim 1/m^\nu$ with $\nu \in [0.3, 0.5]$ (one has to keep in mind however, that most data were not in the dilute limit and that ν was extracted from a restricted range of variation of m); compared to the previous JV estimate $\lambda_d \propto \Delta/m^{1/4}$, Eq.(17) is thus in better agreement with numerical data.

A very close estimate for λ_d can be derived from PR and S^{info} in the Gaussian domain. Just as $\zeta = \zeta_0$ in Eqs. (10) describes S^{info} and PR in the Gaussian domain,

$$\zeta_0(\lambda) = \sigma_h/\sqrt{\sigma_h^2 + \lambda^2\sigma_V^2} = \sqrt{(f^2\Delta^2)/(f^2\Delta^2 + g^2\lambda^2)}, \quad (18)$$

it is to be expected (by extending in a straight forward manner the arguments in [3] where $h(1)$ basis is considered) that in the $V(2)$ basis also the PR and S^{info} will be given by (10) but with $\zeta = \zeta_\infty$ where,

$$\zeta_\infty(\lambda) = \lambda\sigma_V/\sqrt{\sigma_h^2 + \lambda^2\sigma_V^2} = \sqrt{(g^2\lambda^2)/(f^2\Delta^2 + g^2\lambda^2)} \quad (19)$$

The factors f^2 and g^2 in Eqs. (18,19) are defined in (12). In Fig. 7 it is verified that Eq. (10) with $\zeta = \zeta_\infty$ indeed describes the numerical EGOE(1+2) results. Having demonstrated this, it is easily seen that the obvious condition for S^{info} and PR (also strength functions) to be same in both $h(1)$ and $V(2)$ basis is

$$\zeta_0(\lambda_d) = \zeta_\infty(\lambda_d) \implies \lambda_d = |\Delta f/g|, \quad \zeta^2(\lambda_d) = 0.5 \quad (20)$$

Using Fig. 3 and the condition $\zeta^2(\lambda_d) = 0.5$ gives for the $m = 6, N = 12$ example, $\lambda_d = 0.29$. In the dilute limit, the m dependence of λ_d follows from Eqs. (12,13,20),

$$\lambda_d \sim \Delta/(3m)^{1/2} \quad (21)$$

Thus the Gaussian domain arguments give ν (in $\lambda_d \sim 1/m^\nu$) to be 0.5 unlike the improved BW domain arguments (Eq. (17)) giving 0.375. With λ_d defined, a much more significant result that follows from (18-20) is $\zeta_\infty(\lambda) = \zeta_0(\lambda_d^2/\lambda)$ and thus there is a duality in EGOE(1+2), i.e. the results in $h(1)$ and $V(2)$ basis are related to each other by the duality transformation $\lambda \rightarrow \lambda_d^2/\lambda$. As stated before, the same transformation is also derived by JV but using Γ_k and ξ_2 in the BW domain and this points-out its general validity. Strictly speaking λ_d does not lie in the BW domain nor deep into the Gaussian domain. The duality transformation is well tested in Fig. 8 for $F_k(E)$ and in Fig. 9 for $S^{\text{info}}(E)$. In these calculations $\lambda_d = 0.29$. It should be recognized that for the strength functions in Fig. 8, the variances are ζ_0^2 and ζ_∞^2 in the $h(1)$ and $V(2)$ basis respectively. In the case of $S^{\text{info}}(E)$ one sees (from Fig. 9) departures, for $F_k(E)$ close to Gaussian, in the region well away from the centroid of E and this could be because the tails of $F_k(E)$ display exponential localization [14, 33]. These disagreements are not seen in [19] as in this work only $S^{\text{info}}(E = 0)$ and $\xi_2(E = 0)$ are studied. It is useful to point-out that there appears to be a close relationship between λ_d and thermodynamics of finite quantum systems. Using the Gaussian domain formulas (see [20]) for the thermodynamic, information and single particle entropies, it is easily verified that at and around λ_d , all the three entropies will be very close to each other; numerical verification of this result is given in [20]. Therefore it is possible to define the region around λ_d as ‘thermodynamic region’ for interacting particle systems as here different definitions of thermodynamic quantities like entropy will give same results; see [20, 34].

VI. CONCLUSIONS

In this paper an attempt is made to bring completion to the analytical (in BW and Gaussian domains) and numerical investigations, initiated by a number of research groups, of EGOE(1+2) random matrix model for finite interacting quantum systems. Towards this end, a function describing the BW to Gaussian transition in strength functions is identified (Eq. (4)) and it is used to study participation ratio and information and structural entropy as a function of the interaction strength. Also it is shown, using Gaussian domain results, that the duality point λ_d behaves more like $\lambda_d \sim 1/\sqrt{m}$ where m is number of fermions. Applications of these results are given for the BW to Gaussian transition in the series of neutral atoms CeI, PrI, NdI, PmI and SmI. As for EGOE(1+2), what remains is a rigorous analytical treatment of this random matrix model. This will give for example a theory for α vs λ (see Fig. 2), a theory for S^{info} and PR in the $\lambda \lesssim \lambda_c$ domain etc. Finally it is important to remind that only recently rigorous analytical treatment has started becoming available for the simpler EGOE(2) [23].

Acknowledgments

Thanks are due to Ph. Jacquod for a careful reading of the first draft of the paper and for making many suggestions for improving it. The present work was initiated as a result of the correspondence one of the authors (VKBK) have had with Ph. Jacquod. Thanks are also due to Imre Varga for correspondence in the initial stages of this work.

-
- [1] V.K.B. Kota, Phys. Rep. **347**, 223 (2001).
 - [2] T.A. Brody, J. Flores, J.B. French, P.A. Mello, A. Pandey, and S.S.M. Wong, Rev. Mod. Phys. **53**, 385-479 (1981).
 - [3] V.K.B. Kota and R. Sahu, Phys. Rev. E **64**, 016219 (2001).
 - [4] J.M.G. Gómez, K. Kar, V.K.B. Kota, J. Retamosa, and R. Sahu, Phys. Rev. C **64**, 034305 (2001); V. Velázquez and A.P. Zuker, Phys. Rev. Lett. **88**, 072502 (2002); M. Horoi, J. Kaiser, and V. Zelevinsky, Phys. Rev. C **67**, 054309 (2003); V.K.B. Kota, Ann. Phys. (N.Y.) **306**, 58 (2003).
 - [5] V.V. Flambaum, A.A. Gribakina, G.F. Gribakin, and I.V. Ponomarev, Physica D **131**, 205 (1999); V.V. Flambaum, A.A. Gribakina, G.F. Gribakin, and C. Harabati, Phys. Rev. A **66**, 012713 (2002).
 - [6] Dilip Angom and V.K.B. Kota, Phys. Rev. A **67**, 052508 (2003).
 - [7] X. Leyronas, P.G. Silvestrov, and C.W.J. Beenakker, Phys. Rev. Lett. **84**, 3414 (2000); Ph. Jacquod and A.D. Stone, Phys. Rev. Lett. **84**, 3938 (2000); Phys. Rev. B **64**, 214416 (2001).
 - [8] Y. Alhassid, Ph. Jacquod, and A. Wobst, Phys. Rev. B **61**, R13357 (2000), Physica **E9**, 393 (2001); Y. Alhassid and A. Wobst, Phys. Rev. B **65**, 041304 (2002).
 - [9] T. Papenbrock, L. Kaplan, and G.F. Bertsch, Phys. Rev. B **65**, 235120 (2002).
 - [10] M. Mézard, G. Parisi, and M.A. Virasoro, Spin Glass Theory and Beyond (World Scientific, Singapore, 1987).
 - [11] B. Georgeot and D.L. Shepelyansky, Phys. Rev. E **62**, 3504 (2000); **62**, 6366 (2000); G. Benenti, G. Casati, and D.L. Shepelyansky, Euro. Phys. J. **D17**, 265 (2001); V.V. Flambaum and F.M. Izrailev, *ibid.* **64**, 026124 (2001).
 - [12] V.K.B. Kota and K. Kar, Phys. Rev. E **65**, 026130 (2002).
 - [13] V.V. Flambaum, G.F. Gribakin, and F.M. Izrailev, Phys. Rev. E **53**, 5729 (1996).
 - [14] V.V. Flambaum and F.M. Izrailev, Phys. Rev. E **56**, 5144 (1997).
 - [15] S. Åberg, Phys. Rev. Lett. **64**, 3119 (1990).
 - [16] Ph. Jacquod and D.L. Shepelyansky, Phys. Rev. Lett. **79**, 1837 (1997).
 - [17] B. Georgeot and D.L. Shepelyansky, Phys. Rev. Lett. **79**, 4365 (1997).
 - [18] V.V. Flambaum and F.M. Izrailev, Phys. Rev. E **61**, 2539 (2000); V.K.B. Kota and R. Sahu, preprint nucl-th/0006079.
 - [19] Ph. Jacquod and I. Varga, Phys. Rev. Lett. **89**, 134101 (2002).
 - [20] V.K.B. Kota and R. Sahu, Phys. Rev. E **66**, 037103 (2002).
 - [21] M.L. Mehta, Random Matrices, 2nd edition (Academic Press, New York, 1991).
 - [22] Ph. Jacquod and D.L. Shepelyansky, Phys. Rev. Lett. **75**, 3501 (1995).
 - [23] L. Benet, T. Rupp, and H.A. Weidenmüller, Phys. Rev. Lett. **87**, 010601 (2001); Ann. Phys. (N.Y.) **292**, 67 (2001); Z. Pluhar and H.A. Weidenmüller, Ann. Phys. (N.Y.), **297**, 344 (2002).
 - [24] A. Stuart and J.K. Ord, Kendall's Advanced Theory of Statistics, fifth edition of Volume 1: Distribution Theory (Oxford University Press, New York, 1987).
 - [25] I. Varga and J. Pipek, Phys. Rev. E **68**, 026202 (2003).

- [26] M. Abramowitz, I.A. Stegun (Eds.), Handbook of Mathematical functions, NBS Applied Mathematics Series, Vol. 55, U.S. Govt. Printing Office, Washington, D.C. (1964).
- [27] A. Cummings, G. O'Sullivan, and D. M. Heffernan, *J. Phys.* **B34**, 3407 (2001).
- [28] Angom Dilip, I. Endo, A. Fukumi, M. Linuma, T. Kondo, and T. Takahasi, *Euro. Phys. J.* **D14**, 271 (2001).
- [29] M. Sekiya, K. Narita, and H. Tatewaki, *Phys. Rev. A* **63**, 012503 (2001).
- [30] I. P. Grant and H. M. Quiney, in *Advances in Atomic and Molecular Physics*, Vol 23, edited by D. Bates and B. Bederson (Academic Press, New York, 1987) p. 37.
- [31] F. Parpia, C. Fischer, and I. Grant, *Comput. Phys. Commun.* **94**, 249 (1996).
- [32] Ph. Jacquod, private communication (2003).
- [33] N. Frazier, B.A. Brown, and V. Zelevinsky, *Phys. Rev. C* **54**, 1665 (1996); W. Wang, F.M. Izrailev, G. Casati, *Phys. Rev. E* **57** (1998) 323.
- [34] M. Horoi, V. Zelevinsky, and B.A. Brown, *Phys. Rev. Lett.* **74**, 5194 (1995).

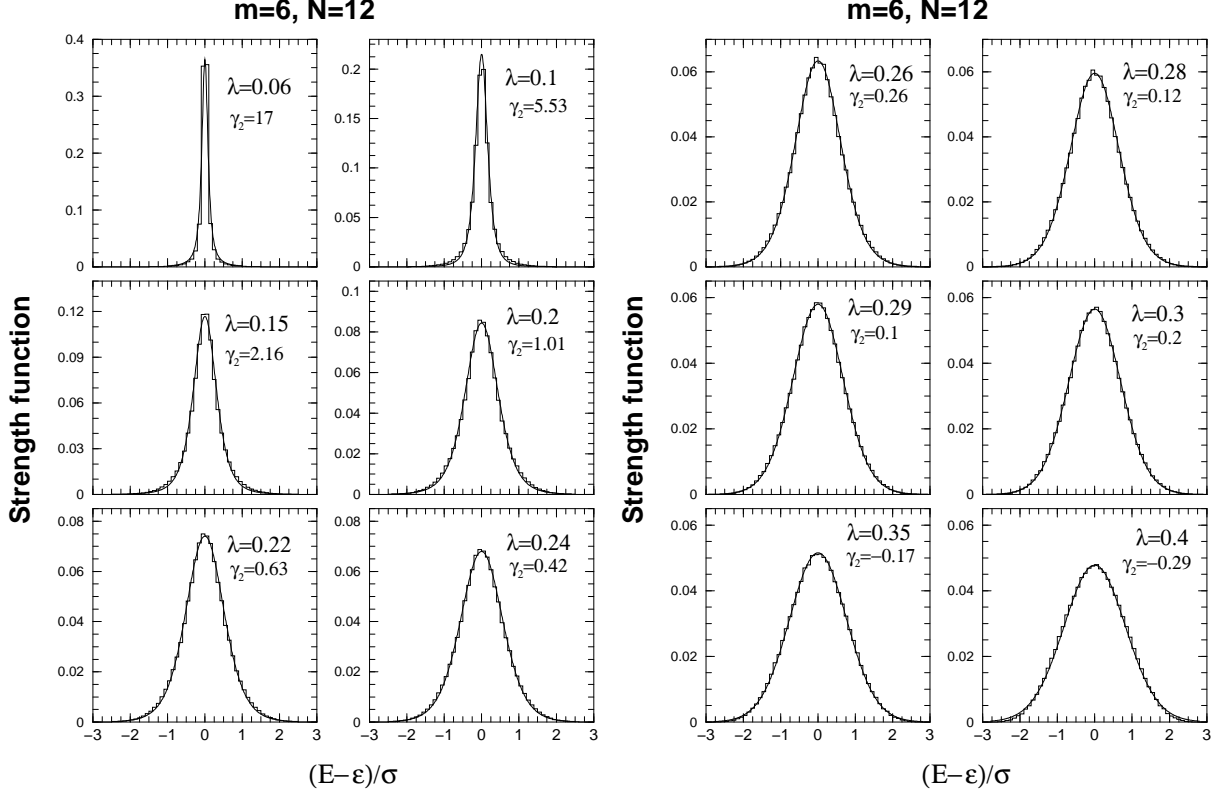


FIG. 1: Strength functions $F_k(E)$ for a 20 member EGOE(1+2) for various values of the interaction strength λ in $\{H\} = h(1) + \lambda\{V(2)\}$ for a system of 6 fermions in 12 single particle states; the matrix dimension is 924. The single particle energies used in the calculations are $\epsilon_i = (i + 1/i)$, $i = 1, 2, \dots, 12$ just as in [1]. In the figures $F_k(E)$ is plotted against $\hat{E} = (E - \epsilon)/\sigma$ where ϵ is the spectrum centroid and σ is the width. The histograms are EGOE(1+2) results and the continuous curves are the best fit $F_{k:BW-G}(E)$ from Eq. (4). In constructing the strength functions, $|C_k^E|^2$ are summed over the basis states $|k\rangle$ in the energy window $\hat{E}_k \pm \Delta$ and then the ensemble averaged $F_{\hat{E}_k}(\hat{E})$ vs \hat{E} is constructed as a histogram; the value of Δ is chosen to be 0.05 for $\lambda = 0.06$ and beyond this $\Delta = 0.1$. Here $\hat{E}_k = (E_k - \epsilon_H)/\sigma_H$ and in the figures results shown for $F_k(E)$ with $\hat{E}_k = 0$. Similar results are also obtained for the $(m = 7, N = 14)$ system.

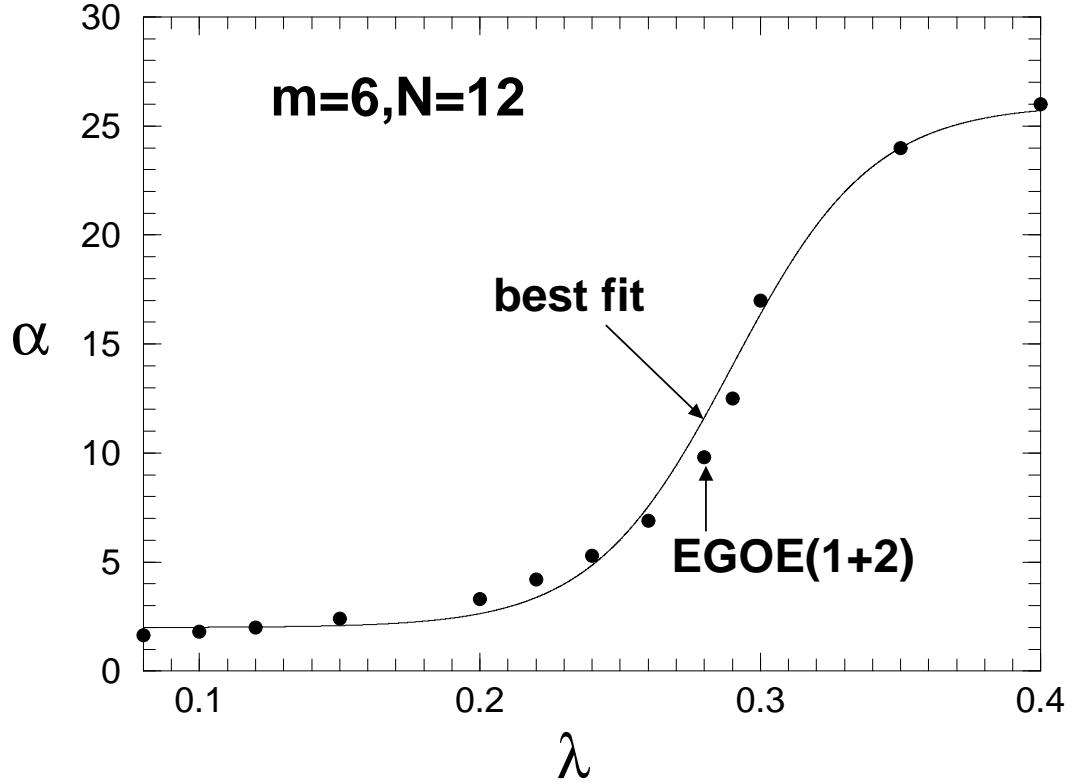


FIG. 2: For $\lambda \geq 0.08$, α vs λ obtained by fitting the $F_k(E)$ in $h(1)$ basis to the interpolating form $F_{k:BW-g}$ given by (4). Results are shown for the EGOE(1+2) system used in Fig. 1. The filled circles give the best fit α values and the continuous curve, given by $\alpha = 24/[exp - (40(\lambda - \lambda_0)) + 1] + 2$ with $\lambda_0 = 0.29$, guides the eye. It is curious to note that λ_0 is close to λ_d , the duality point discussed in Section 5. Similar results are also obtained for the ($m = 7, N = 14$) system.

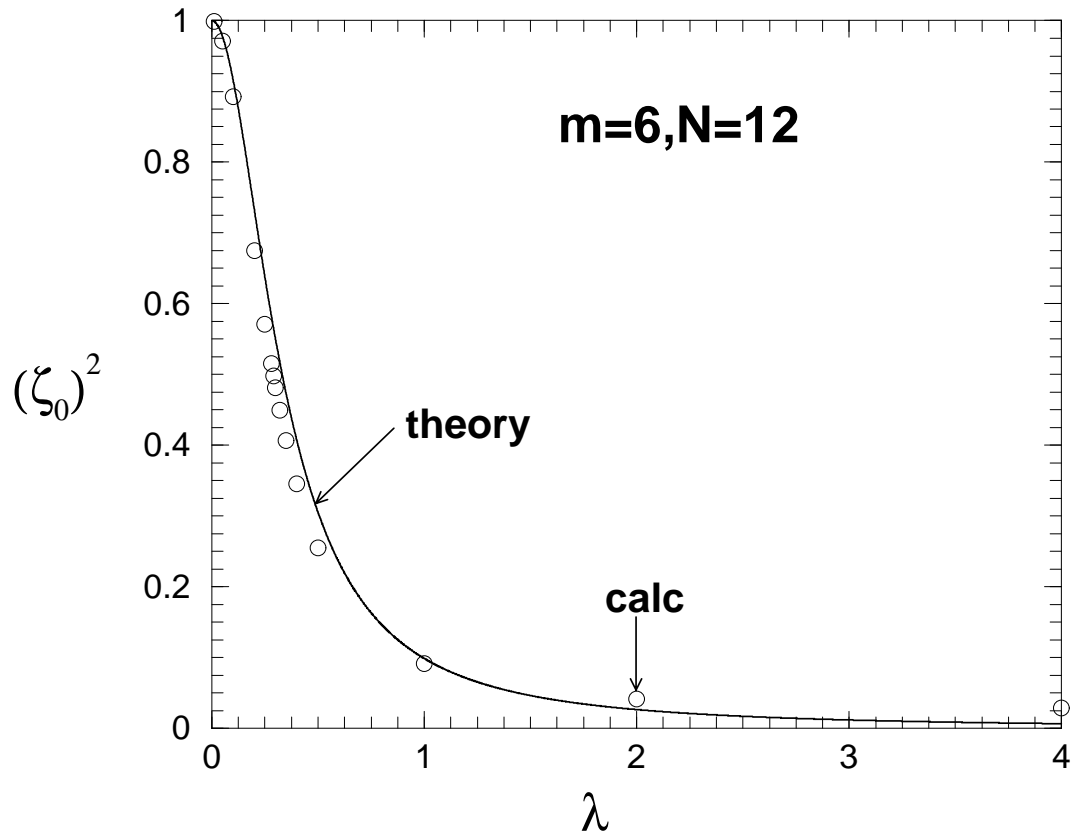


FIG. 3: Square of the correlation coefficient ζ_0^2 vs λ for the EGOE(1+2) system used in Fig. 1. Theoretical results (continuous curve) given by (11,12) are compared with the numerical EGOE(1+2) results (open circles).

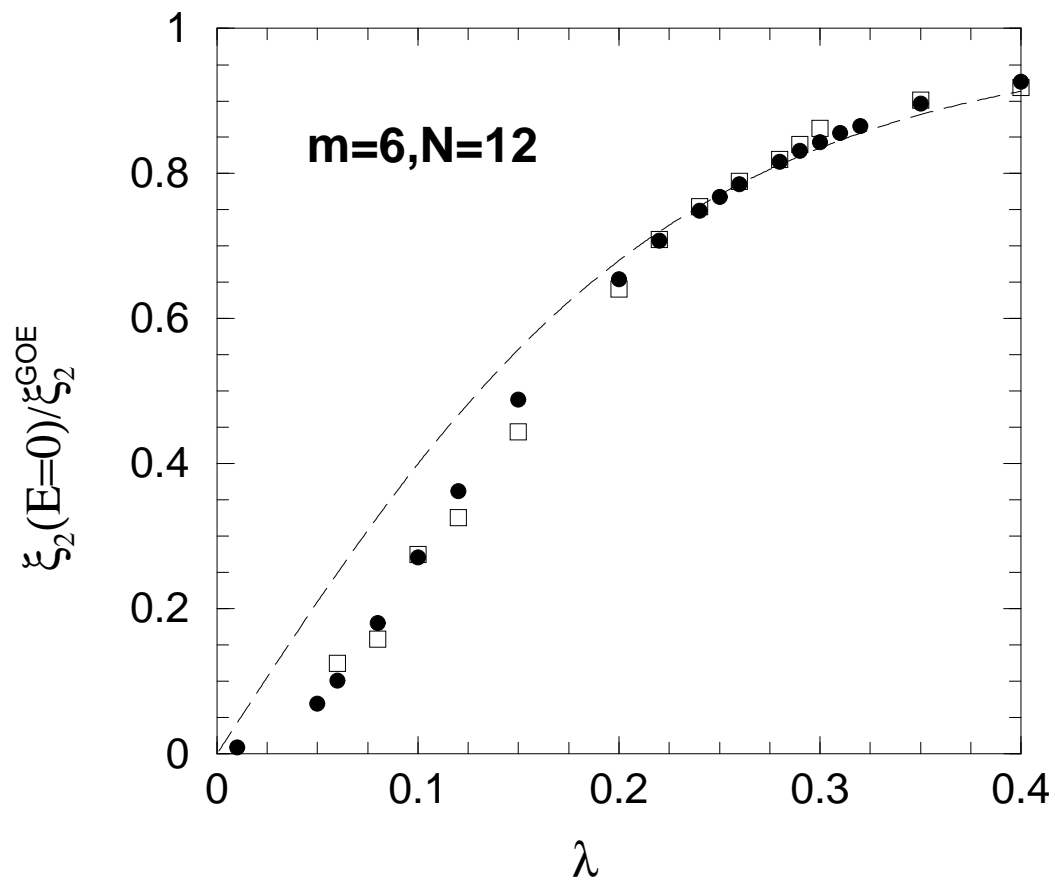


FIG. 4: Participation ratio $\xi_2(E=0)/\xi_2^{GOE}$ vs λ for the EGOE(1+2) system used in Fig. 1. Theoretical results given by (14) (open squares) are compared with the EGOE(1+2) results (filled circles). For comparison, the Gaussian domain result (dashed curve) from (10) is also shown.

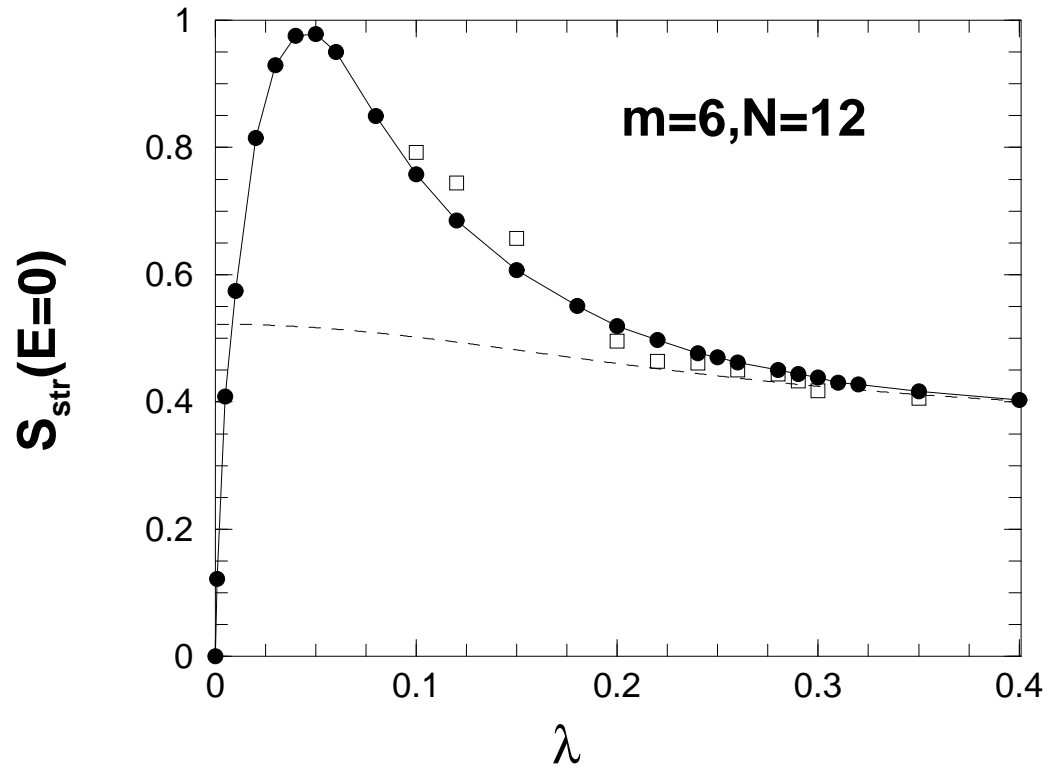


FIG. 5: Structural entropy $S_{\text{str}}(E=0)$ vs λ for the EGOE(1+2) system used in Fig. 1. Theoretical results given by (14,8) (open squares) are compared with the EGOE(1+2) results (filled circles). For comparison, the Gaussian domain result (dashed curve) from (16) is also shown.

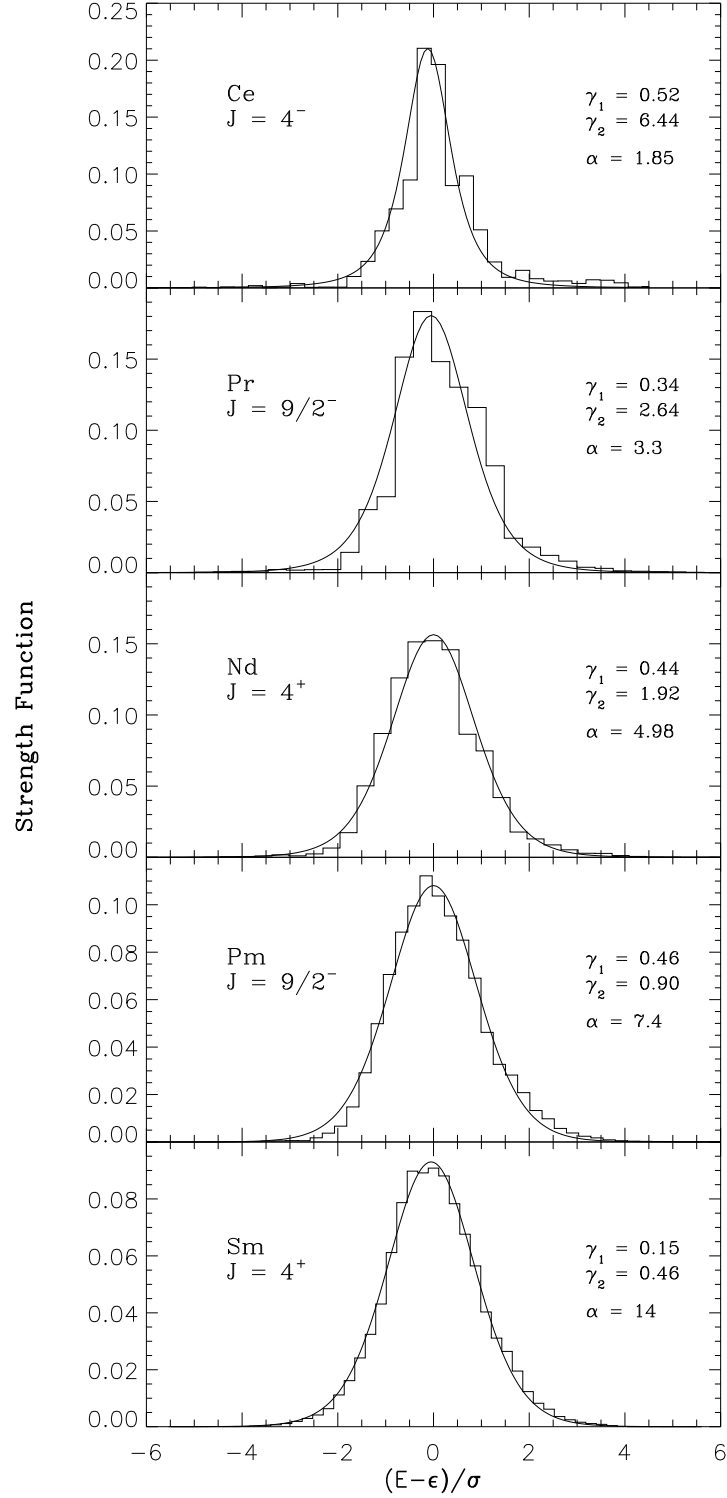


FIG. 6: Strength functions $F_k(E)$ for CeI to SmI. Histograms are calculated strength functions and the smooth curves are $F_{k:BW-G}(E)$. Also given in the figure are the calculated γ_1 (skewness) and γ_2 (excess) values and the deduced values, from the best fits, of α characterizing $F_{k:BW-G}(E)$.

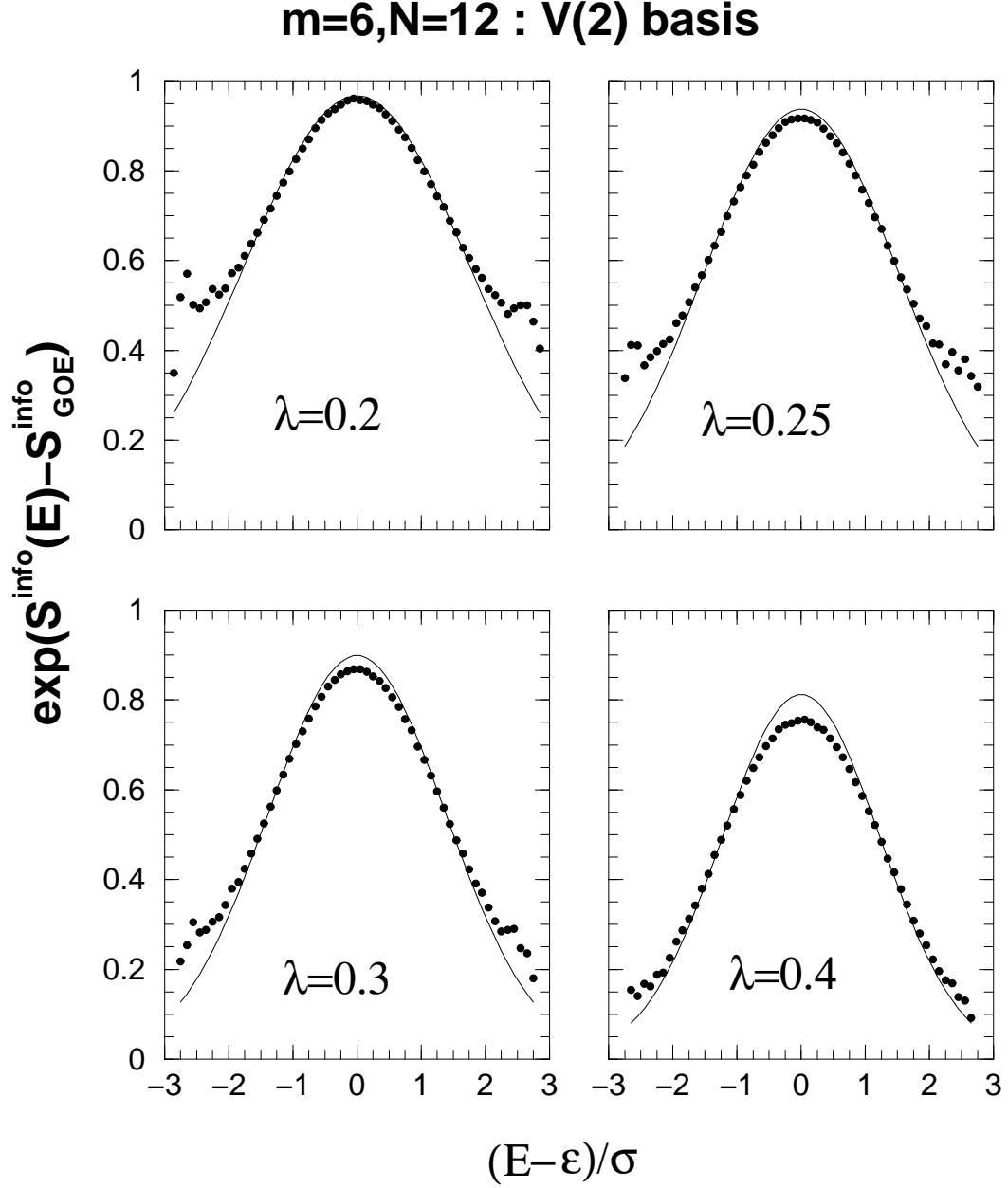


FIG. 7: $\exp(S^{\text{info}}(E=0) - S_{\text{GOE}}^{\text{info}})$ in V(2) basis (filled circles) for four different λ values for the EGOE(1+2) system used in Fig. 1. The continuous curve is from Eq. (10) with $\zeta = \zeta_\infty$.

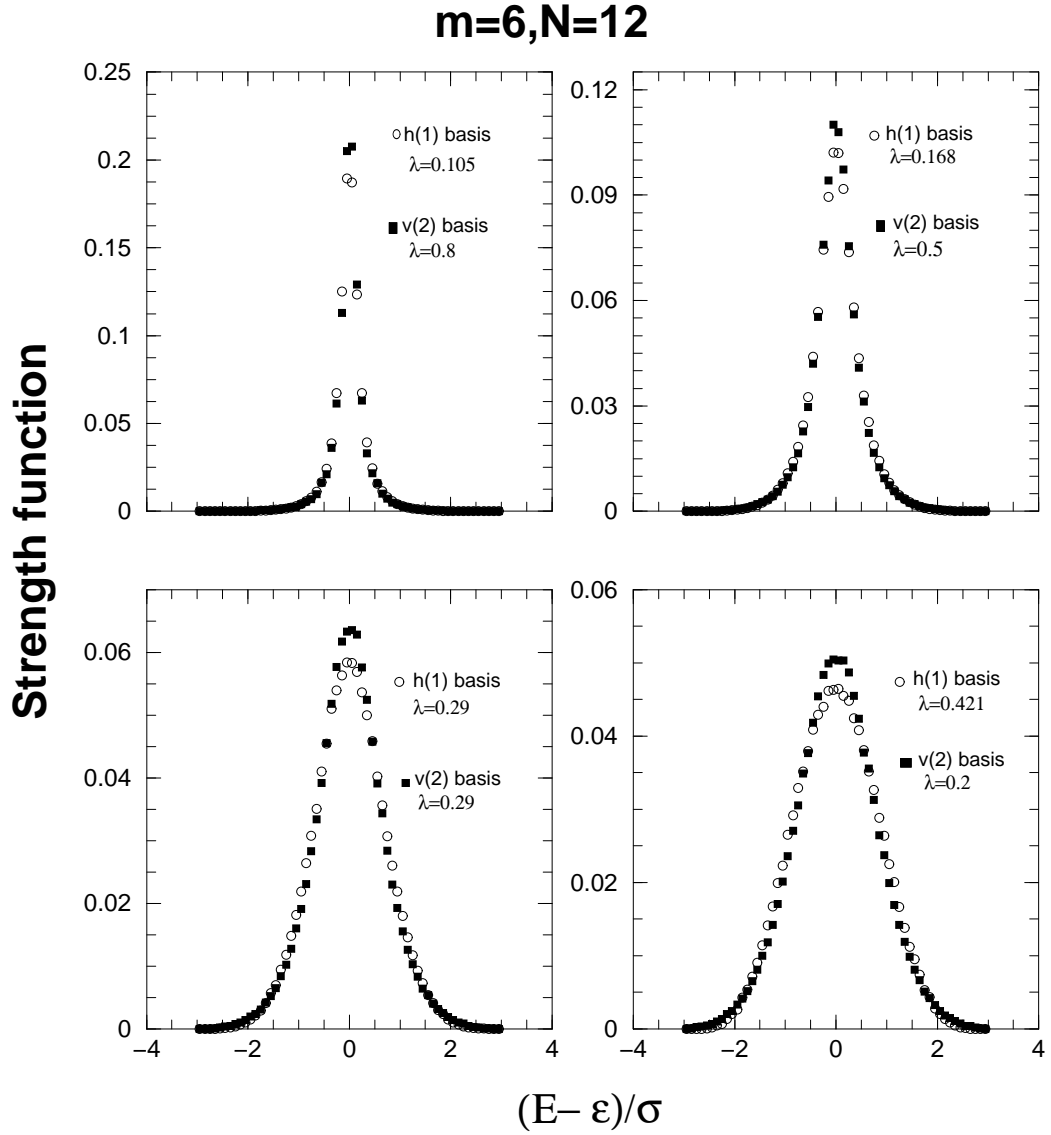


FIG. 8: Strength functions $F_k(E)$ in the $h(1)$ and $V(2)$ basis for four λ values related by the duality transformation $\lambda \rightarrow \lambda_d^2/\lambda$. Results are for the EGOE(1+2) system used in Fig. 1. Here $\lambda_d = 0.29$. Similar results for the BW spreading widths are given in [19] for several EGOE(1+2) systems with $h(1)$ also chosen to be random.

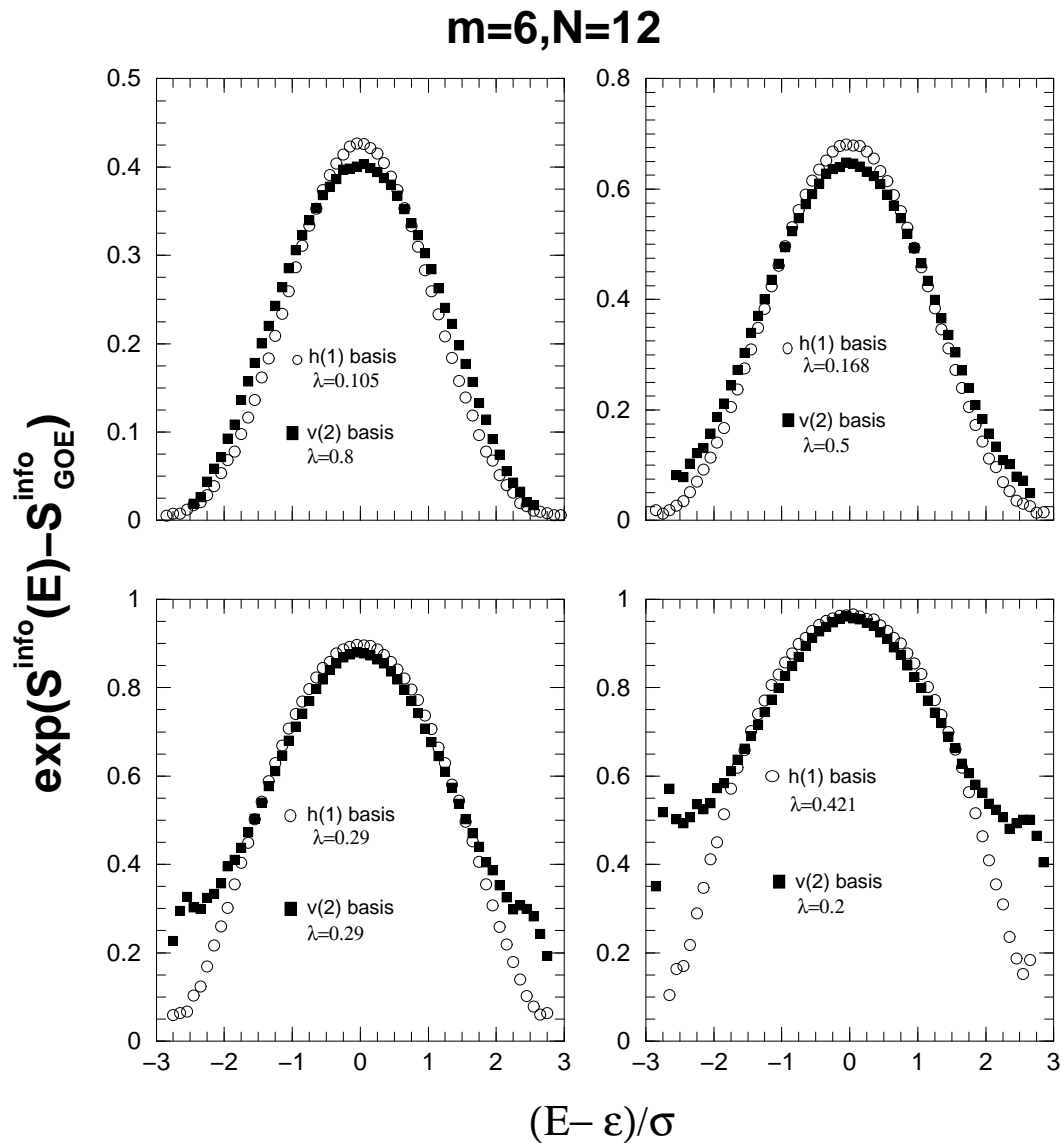


FIG. 9: Same as Fig. 7 but for $\exp(S^{\text{info}}(E) - S_{\text{GOE}}^{\text{info}})$. Similar results for ξ_2 but only at $E = 0$ are given in [19].